

Review

Plasma-Driven Sciences: Exploring Complex Interactions at Plasma Boundaries

Kenji Ishikawa ^{1,*} , Kazunori Koga ²  and Noriyasu Ohno ¹ ¹ Center for Low-Temperature Plasma Sciences, Nagoya University, Nagoya 454-8601, Japan² Faculty of Information Science and Electrical Engineering, Kyushu University, Fukuoka 819-0395, Japan

* Correspondence: ishikawa.kenji@nagoya-u.jp

Abstract: Plasma-driven science is defined as the artificial control of physical plasma-driven phenomena based on complex interactions between nonequilibrium open systems. Recently, peculiar phenomena related to physical plasma have been discovered in plasma boundary regions, either naturally or artificially. Because laboratory plasma can be produced under nominal conditions around atmospheric pressure and room temperature, phenomena related to the interaction of plasma with liquid solutions and living organisms at the plasma boundaries are emerging. Currently, the relationships between these complex interactions should be solved using science-based data-driven approaches; these approaches require a reliable and comprehensive database of dynamic changes in the chemical networks of elementary reactions. Consequently, the elucidation of the mechanisms governing plasma-driven phenomena and the discovery of the latent actions behind these plasma-driven phenomena will be realized through plasma-driven science.

Keywords: plasma-driven sciences; plasma processing; plasma-wall interactions; plasma agriculture; plasma seed science



Citation: Ishikawa, K.; Koga, K.; Ohno, N. Plasma-Driven Sciences: Exploring Complex Interactions at Plasma Boundaries. *Plasma* **2024**, *7*, 160–177. <https://doi.org/10.3390/plasma7010011>

Academic Editor: Andrey Starikovskiy

Received: 29 December 2023

Revised: 31 January 2024

Accepted: 19 February 2024

Published: 27 February 2024



Copyright: © 2024 by the authors. Licensee MDPI, Basel, Switzerland. This article is an open access article distributed under the terms and conditions of the Creative Commons Attribution (CC BY) license (<https://creativecommons.org/licenses/by/4.0/>).

1. Introduction

In the universe, space is filled with matter that interacts electromagnetically [1,2] with the remaining unresolved energy. As matter is energetically excited, excited states involving electrons and ions are formed from particles in the ground state. The collection of ionized matter is known as plasma [3,4]. The plasma state can be found naturally or artificially in various situations.

Plasma phenomena have been studied in the natural sciences in subjects such as cosmic plasma physics, astrophysics, atmospheric physics, and chemistry, as well as laboratory plasmas such as laser-produced plasma and magnetically confined plasma to create fusion energy. The central region is a high-temperature plasma surrounded by the boundary region that forms a low-temperature plasma (LTP) and, upon detaching, usually flows toward the edge and generates secondary plasma processes at the boundary (Figure 1). At the boundary, secondary processes involve plasma-induced molecular dissociations providing electronically neutral particles called radicals, which are chemically reactive and often have unpaired electrons [5]. The chemically rich reaction field artificially produces interactions between plasma-generated particles, such as electrons, ions, radicals, and photons, which are triggered by electron collision-induced reactions. Plasma processes at the boundary layer are critical and are observed in various fields [6–8], such as film deposition and material etching, plasma medicine, plasma agriculture, and plasma pharmacy. In the interactions of plasma with solid-state materials, liquids, and living organisms, the mechanisms explaining these mysterious phenomena have not yet been comprehensively clarified. The unique characteristics of the LTP technology are the nonequilibrium nature of temperature-independent chemical reactions and the fact that artificial plasma generation mimics the chemistry-rich and nonlinear dynamic nature of physicochemical reactions.

Here, we envision the future of plasma-driven science and highlight the emergence of studies that unravel the interactions between complex plasma systems and other phases. Mysteries regarding plasma are being solved using contemporary science within the peculiar phenomena driven by plasma and the discovery of latent actions is underway. This review first introduces the fundamental aspects of plasma in natural sciences and then describes developments in emerging fields. By combining knowledge of plasma physics with that of plasma chemistry, these disciplines have emerged as LTP science and technology. A new academic discipline based on plasma-driven science has been established.

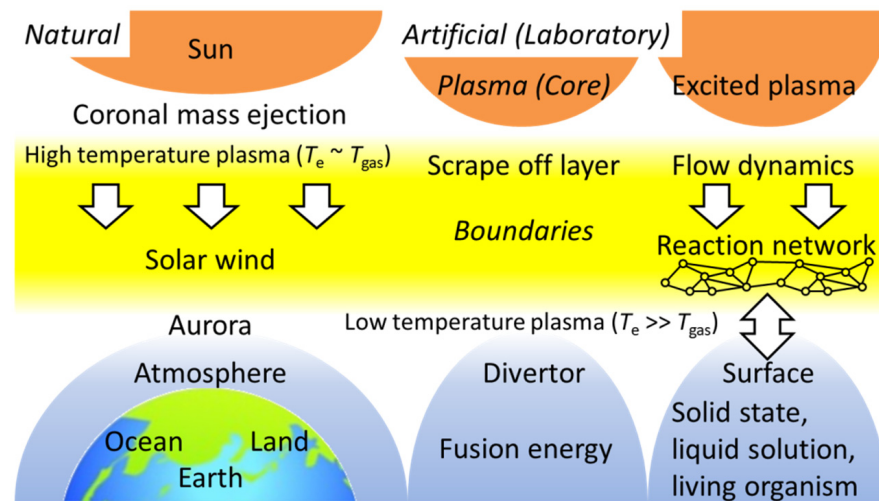


Figure 1. Plasma boundaries for the complex interaction of natural (left) and artificial (right) plasma-related phenomena. Complex interactions between the systems occur at the interfaces when facing the excited plasma to the counter surface for solid-state materials, liquid solutions, and living organisms. In the phase boundary surface, plasma generates particles, such as electrons, ions, radicals, and photons, in the excited plasma transport-based flow dynamics and creates a chemical reaction network. As energy flow one direction from the source plasma to surface of matters, Sun–Earth relationship is mimicked to form the plasma boundary regions in cases of various laboratory plasma fields.

2. Fundamental Aspects of Plasma: Collective Phenomena from Micro- to Macroscopic Dynamics

Plasma is the name of a state of matter that is a collection of particles, such as electrons, ions, and neutral gases, and its material phase spans a wide range of densities, n , and temperatures, T . The number density per unit volume was defined separately for each particle in the plasma state as n_e for electrons, n_i for ions, and n_{gas} for background gas. Assuming a Maxwellian distribution, their temperatures, T_e , T_i , and T_{gas} , are used as an indicator of the statistical distribution of the velocity of motion of the particle population individually. Not all cases were in thermal equilibrium with maximum entropy. Note that LTP is defined only by a high electron temperature, with separating gas temperatures at approximately 1000 K in conjunction with high-temperature plasma for nuclear fusion and arc discharges.

The plasma phenomena occurring at the boundary layer, driven by the energy flow from the central regions, exhibit hysteresis and nonlinear behaviors, and these have not yet been solved. The particle velocity of a single particle, v , under a homogenous electromagnetic field can be expressed as $\frac{dv}{dt} = \frac{e}{m}(E + v \times B)$, where E and B are the electric and magnetic field vectors, respectively, e is the elementary charge, and m is the particle mass. A collection of particles behaves as another type of material. In the central core area of the

plasma, the temporal variation in the particle velocity distribution function for the i type of particles, $f^{(i)}(v)$, at time t and position r satisfies Boltzmann's equation [9,10].

$$\frac{df^{(i)}(v)}{dt} + v \cdot \nabla_r f^{(i)}(v) + \frac{e}{m} (\mathbf{E} \times \mathbf{B}) \cdot \nabla_v f^{(i)}(v) = \left. \frac{df^{(i)}(v)}{dt} \right|_{coll}. \quad (1)$$

This indicated that the electromagnetic force sustained a plasma state containing charged electrons and ions.

Hence, the plasma generates a natural electric field potential, creating a sheath region at the boundary with the bulk plasma and adjusting the motion of the charged particles. This spatial length of the potential can be measured by the Debye length, $\lambda_D = \sqrt{\frac{k_b T_e}{e^2 n_e}}$, where k_b is the Boltzmann constant, and n_e is the density of the particle, and together with the Coulomb logarithm parameter $\log \Lambda = \frac{4}{3} \lambda_D^3 n_e$. As electrons are more densely populated and interatomic distance reaches the de Broglie wavelengths, $\lambda_B = \frac{h}{m_e v_e}$, the thermal energy of the electrons, $k_b T = \frac{1}{2 m_e} \epsilon F^2$, becomes equal to the Fermi energy, ϵ_F , and the electrons no longer behave as an isolated particle. In contrast to the isolated particle phenomenon, the collective phenomenon of plasma has attracted attention because of the following characteristics.

Nonlinearity of plasma responses is a consideration. Plasma can be regarded as a dielectric fluid because an electromagnetic wave with higher frequencies than plasma frequency, $\omega_p = \sqrt{\frac{q^2 n_e}{\epsilon_0 m_e}}$, transmits through bulk plasma as a dielectric medium. The polarization fields, P , develop by a linear response of the applying electromagnetic field strengths; $\mathbf{P} = \hat{\epsilon}_p \mathbf{E}$. This implies that the plasma can be described by the superposition of a collection of microscopic polarization of each particle. When the field strength is beyond the range of the linear response, the system no longer responds linearly, because the interrelationship among the motions of individual particles cannot be ignored. Therefore, plasma exhibits plasticity and its dynamic changes are irreversible.

Hysteresis of plasma quantities is also a consideration. In the case of atmospheric-pressure plasma, one example is presented where the density levels of relatively long-lived, vibrationally excited, and metastable-state species are dependent on the impurities of humid air and repetition rates of plasma excitations because of the contribution of Penning ionization via excited metastable particles [11,12]. The rare gas metastable atom density modifies the ignition properties of the pulsed-operated plasma. This can be regarded as the hysteresis behavior of the plasma media, for instance, the phases parameterized by the density of metastable atoms and occupation of higher rovibrational levels. The densities of the metastable species depend on the hysteretic manner with a balance of generation and losses via collision-induced reactions among electrons, neutrals, ions, and metastables. Thus, the microscopic energy balance between gains and losses determines the type of plasma compositional phase that reflects the state.

A statistical collection of microscopic particles satisfies more naturally the phenomenological Landau theory with the order parameter, η , and minimizes its macroscopic free energy, $(T, \eta) = \min \left\{ F_0 + \frac{k_1}{2} \eta^2 + \frac{k_2}{4} \eta^4 + \frac{k_3}{6} \eta^6 \dots - \hat{\epsilon}_p \mathbf{E} \right\}$, where k 's are constants and the Gibbs free energy is represented with enthalpy, H , and entropy, S , by $G = H - TS$. Accordingly, the gain and loss of energy by ordering the structure and thermal motion were balanced and reached an equilibrium state.

Similar to ferroelectrics, T_c , the phase is an ordinary dielectric at temperatures higher than the critical temperature and moves its phase with permanent polarization at temperatures lower than T_c , called the ferroelectric phase. Such phase transitions are also created by the statistical ordering of collective phenomena.

Furthermore, the time evolution of canonical systems has been described using Liouville's theorem with probability functions in statistical mechanics. From this, a state in the time-step process responds stochastically to the next state, which is deterministic with a probability function from a unique state of the previous step. This is called the Markov

process. However, in addition to the random Brownian process, plasma hysteresis may be invoked by the probabilistic and nonstationary nature of non-Markov processes.

Nonequilibrium three behaviors of plasma is the last consideration. When the plasma is enclosed by a boundary, its energy dissipates continuously from the core to the edge. Conversely, interactions occurring at the boundary are characteristic. Thermodynamically, the system relaxes toward a stable state. Under these circumstances, both the energy input and relaxation of the plasma system should be considered. When a system is kinetically unstable, its transient behavior can be measured. First, temporal changes in the system variables occur owing to the energy input as well as a balance of the energy inputs and relaxations. By breaking this balance, the system variables move toward an equilibrium state. Second, multiple species are thermally discrepant; that is, there are temperature differences among electrons, ions, and neutral species. The thermodynamic properties are statistically in nonequilibrium, far from the Maxwell–Boltzmann distribution. The above-mentioned nonequilibrium should be recognized by kinetic, thermodynamic, and chemical equalizations. At the boundary of the plasma, excited particles continuously impinge on the surface and collide with the boundary materials. This leads to a nonequilibrium state called the formation of physicochemical reaction fields.

The points of nonlinearity, hysteresis, and nonequilibrium for both bulk plasma and the plasma-driven phenomena that occur at the boundary regions of the plasma should be considered. At lower temperatures for electrically neutral gases and heavy mass particles of ions than for charged particles of electrons and ions, this LTP state can be applied to both liquid solutions without boiling and to living organisms without killing them [13], resulting in plasma physics meeting plasma chemistry.

3. Excitation and Relaxation Schemes in the Plasma

3.1. Irreversible Plasma Energy

The plasma was sustained in its excited state by the energy input. Therefore, when the energy input is turned off, the plasma moves toward extinction. The excited plasma system subsequently dissipates energy by de-excitation or recombination of the charged particles and so forth. Interestingly, electron impact reactions, such as ionization, dissociation, excitation, and electron attachment, are induced when energetic electrons collide with atoms and molecules in the bulk plasma. The recombination process produces heat and is formed by a thermodynamic cycle of excitation during discharge and de-excitation by radiation loss and recombination, and is referred to as the “primary relaxation process” and the first detachment.

Irreversibly, the production of chemically active species and radicals generated by collisions between the excited plasma particles and the background neutral particles is referred to as the “secondary relaxation process”, the second detachment, and the detached recombining plasma.

Irreversibility measures the degree of dissociation and is defined as the ratio of the number of dissociated species to the total number of species. For example, nitrogen molecules dissociate into nitrogen atoms with densities $[N_m]$ and $[N_a]$. If the dissociation reaction $N_2 \rightarrow 2 N$ is thermodynamically the reverse reaction, the thermal equilibrium then determines the dissociation degree of a ratio of $[N_a]/[N_m]$ at a constant pressure. If electron-collision-induced dissociation dominates the plasma, the degree of dissociation increases. These processes can be divided into two pathways. The first is a reversible thermodynamic cycle known as the Carnot cycle. The other is an irreversible non-equilibrium pathway, which is often observed in open systems (Figure 2). Note that the cycles are represented depending on the temperature changes of the species. The first simple excitation and detachment cycle is the generalized statistical entropy of the system. The second dissociative open cycle can be measured by the Gibbs statistical entropy, S , obtained by the integral over all i -th microsystem states, $S = -k_b \sum_i p_i \ln p_i$, where p stands for the probability of the molecular-level states with positions and momenta.

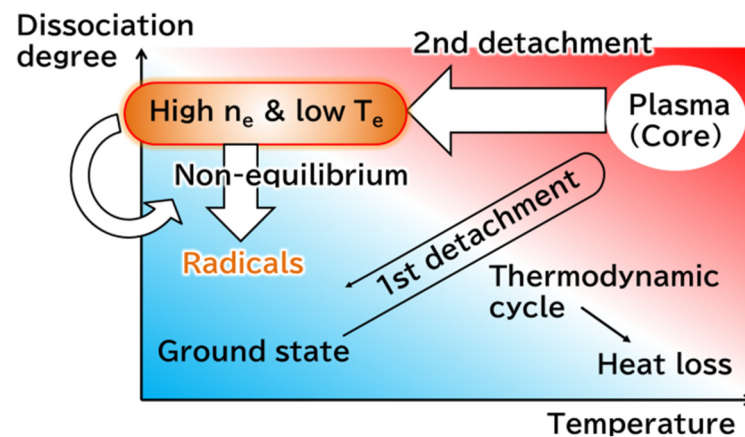


Figure 2. Schematic of the phase diagram of the recombining detached plasma as a function of temperature and dissociation degree of molecular gas. The thermodynamic Carnot cycle exchanges energies along excitation and deexcitation lines with heat loss. The nonequilibrium pathway is evolved by transporting from the high-density core plasma to the boundary with the relaxation of electrons selectively via molecular dissociation processes and forming the detaching recombining detached plasma. Consequently, rich radical reaction fields are provided through the secondary recombination pathway.

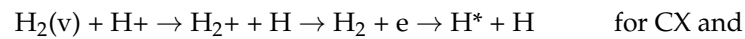
3.2. Recombining Detached Plasma

At the plasma boundary in the peripheral plasma of fusion reactors, during a gas puff of nitrogen, a high density of nitrogen atoms can be generated by driving the transport of excited species extruded from the core plasma. Based on this characteristic, this is called “recombining detached plasma”. Research has been conducted on the use of laboratory plasma for nuclear fusion.

In magnetically confined torus plasma, a divertor is installed to exhaust impurities, such as helium, produced by the fusion reaction in the core plasma out of the reactor [14]. Charged particles entering the divertor from the core plasma become neutral gases via surface recombination on the plasma-facing wall (divertor plate) and are exhausted; however, the divertor plate is subjected to a large heat load. Because divertor plates are subjected to high heat loads, heat removal is necessary. To achieve this, volume recombination is promoted before the ions and electrons enter the divertor plates to reduce heat flux. This is called a detached recombining plasma, as mentioned earlier [15]. When the electron temperature falls below 1 eV, the reaction rate coefficient of three-body recombination becomes larger than that of ionization, and hydrogen ions recombine with electrons to form hydrogen atoms and neutralize them. This process is known as volume electron–ion recombination (VR). However, when nitrogen gas is introduced into the divertor after molecular hydrogen ions are ionized by charge exchange with hydrogen atoms, collisions with nitrogen produce hydrogenated nitrogen molecular ions, which recombine with electrons to annihilate the plasma. The recombination process involving molecules is known as molecular-assisted recombination.

The dissociation cross-section of nitrogen molecules due to electron collisions is larger than that of rare gases, such as Ar and Ne [16]. Hydrogen atoms transfer molecular hydrogen to produce molecular hydrogen ions via charge–exchange reactions. Molecular hydrogen ions recombine with electrons via dissociative recombination to form excited hydrogen atoms. In the other pathway, they recombine with nitrogen molecules via proton transfer to form nitrogen hydride ions. Hydrides recombine with nitrogen molecules via molecule-driven recombination with an electron, forming a hydrogen atom or nitrogen hydrogen and nitrogen atoms [17–19]. Plasma particles and energy transport via convective transport in a detached plasma have been reviewed [15]. For the International Tokamak Experimental Reactor (ITER), reducing the heat load on the divertor plates is important. Generating the detached recombining plasma reduces the heat load on the divertor plates.

Molecule-assisted recombination processes involving molecular hydrogen are classified as charge exchange (CX) and dissociative recombination (DR) [20,21]. The reaction is given by



where $\text{H}_2(v)$ is the vibrationally excited molecular hydrogen and H^* is the excited hydrogen radical. The VR process dominates when the electron temperature in the ionized plasma decreases rapidly over space and time. When the plasma jet is injected into free space, the electron temperature drops, and inelastic collisions in the plasma adiabatically expand, resulting in an afterglow plasma. The plasma is no longer in direct spatial contact with the walls of the vacuum vessel [21]. Thus, the discharge power was abruptly reduced with time (turn-off) to produce plasma at a lower temperature while maintaining density. Specifically, measurements of the electron energy distribution function using laser Thomson scattering have shown a non-Maxwellian distribution function in the time variation of the electron temperature [22,23]. This indicates that the thermal conduction of electrons was faster than the diffusion of ionic particles.

Spatial and temporal measurements of the recombining detached plasma have been conducted [24,25]. Electron density and temperature can be predicted using a machine-learning method for helium emission line intensities in Magnum-PSI [26,27] and PISCES-RF [28]. The prediction precision was improved by modifying the CR model to include the optical escape factor [29].

The complex plasma phenomena of radially ejecting plasma, known as plasma blob-like transport [30], have been analyzed using the three-dimensional spatiotemporal dynamics of detached plasma observed in linear plasma devices, such as NAGDIS [31], PISCES-RF [32], MAGNUM-PSI [33,34], and GAMMA10-PDX [35–37]. The detached recombination process was simulated using the fluid simulation code LINDA considering collisional radiative dielectric recombination [38]. The complex detaching plasma transport was modeled using the feedback instability in the plasma density and the effect of the magnetic flux [39]. A toroidal configuration was tested for detaching plasma at the vacuum vessel wall by cooling the electron temperature as high-density plasma is transported along long spiral magnetic fields [40–43]. Recently, using a long magnetic connection, an electron beam-excited plasma (EBEP) source was developed with both toroidal and vertical magnetic fields, and spiral-shaped nitrogen plasma was successfully produced [43] (Figure 3).

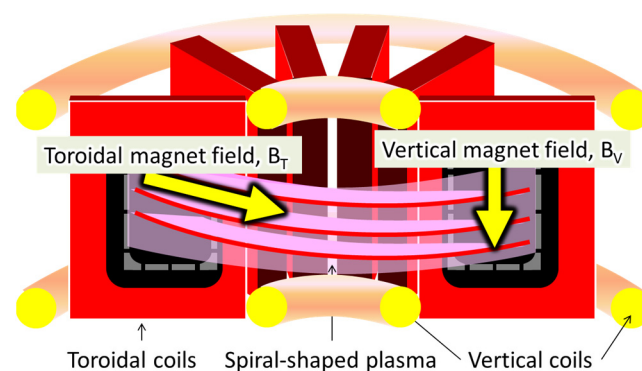


Figure 3. Recent progress of the complex detaching plasma transport: Long magnetic connection with both toroidal and vertical magnet fields sustains a spiral-shaped electron-beam excited plasma of nitrogen. (after Nagase 2007 [40]; Asaoka 2019 [43]).

Understanding and controlling plasma–material interactions can be achieved by dividing the plasma core and peripherals into a hierarchical structure (Figure 1). The hierar-

chy was modeled using multiscale hybrid simulations, as exemplified by the MPEX [44], LINDA [45], kinetic particle-in-cell (PIC) code [46], and scrape-off layer (SOL) PS code [47].

In the core region of the fusion reactors, high-density and high-electron-temperature plasma is generated, and its peripherals are detached from the core plasma by forming “detached recombining plasma,” which is used for nitrogen gas injection into the flow-out hydrogen plasma. The complex motion of the plasma jets was observed.

Similar to the relationship between solar wind and the Earth’s surface, the generated chemical reactions play a versatile role in determining the characteristics of complex plasma–surface interaction fields.

4. Plasma-driven Phenomena

4.1. Artificial Plasma Generation in Nominal Conditions (Temperature and Pressure)

The separation of the gas temperature from the electron temperature is characterized by the arc- and glow-like features at high and low gas temperatures, respectively. Previously, a method was developed to generate stable glow-like plasma under atmospheric pressure without increasing the gas temperature [48–52]. Subsequently, LTP sources have been developed over a long history [53]. High plasma densities and frequent repetitions have been reported [53].

LTP provides a nonequilibrium reaction field for chemically reactive species without thermal heating [13]. Hydrogen plasma chemical reactions can be explained by molecular-activated recombination (MAR) [54]. This study demonstrates the importance of electronically and vibrationally excited state molecules in understanding anomalously fast plasma recombination.

Similarly, nitrogen plasma chemical reactions compete between oxidation and reduction and the nitrogen cycle is relevant to redox reactions (Figure 4). For example, stable dinitrogen can be functionalized with ammonia by forming nitrogen atoms using plasma discharge technology [55–58]. In product life assessments, the circulation of elements such as carbon, nitrogen, and rare metals has become an issue. In situ functionalization of resources can be achieved using plasma-driven catalysts [59,60]. Nitrogen fixation occurs under air and water discharge and can be used as a fertilizer in agriculture [61,62].

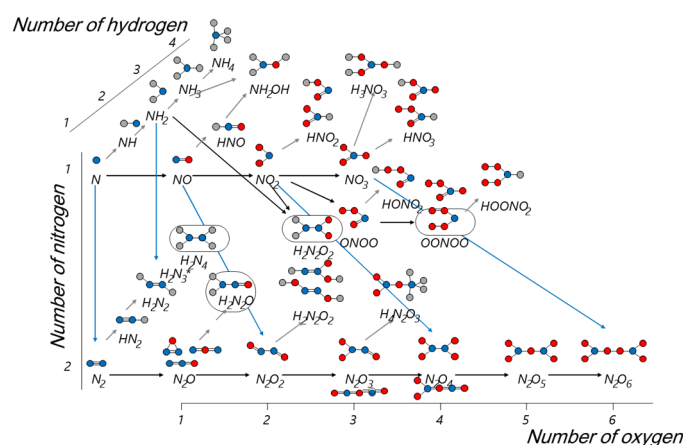


Figure 4. Chart of nitrogen derivatives having the general formula $H_xN_yO_z$, including representative isomers. Red and purple arrows indicate oxidation and hydrogenation, respectively, while gray backgrounds indicate radical or unstable species. A reduced version of the network of chemical reactions is also included here. (Reproduced from Jpn. J. Appl. Phys. 61, SA0802 [60]).

4.2. Emergence of Plasma–Liquid Interactions

Similarly, plasma contacts liquid solutions, and materials are created in them. Plasma–liquid interactions induce some beneficial effects, and the gain of pharmaceutical effectiveness has emerged and is called plasma pharmacy (Figure 5). Eventually, the plasma-contacting liquids kill the cells of living organisms during cultivation in Petri dishes [63].

Comprehensive chemical analyses have shown that plasma-treated liquids contain inorganic reactive species, known as reactive nitrogen and oxygen species (RONS), such as hydrogen peroxide (H_2O_2), nitrous acid (HNO_2), and nitric acid (HNO_3) [64]. The nitrogen-based reactive species, $\text{H}_x\text{N}_y\text{O}_z$, plays a role in the chemical reactions [60] (Figure 4).

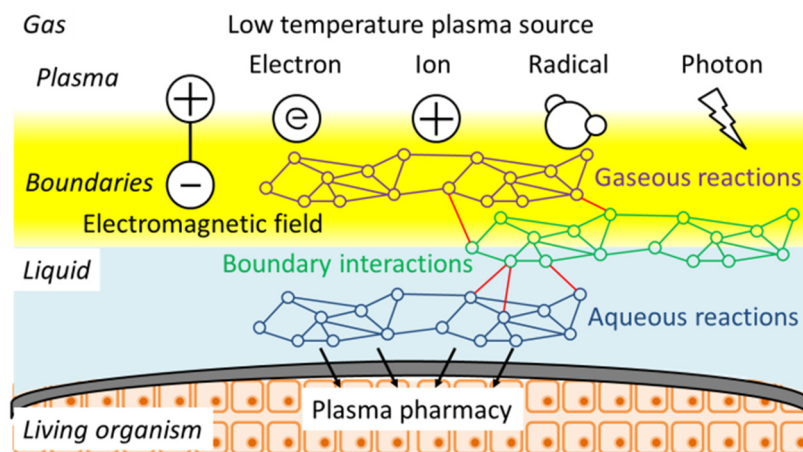


Figure 5. Plasma-pharmacy: The rich chemistry in the plasma-induced aqueous reactions including dehydration, esterification, hydrolysis, and dimerization of the original organic molecules. The chemical reactions can be represented by networks with nodes for reactants and products, and paths for elementary reactions. Hierarchically, the reactions occur across phase boundaries. Reactive species created by multiple reactions on the network are functionalized in situ for biological effectiveness.

A plasma-treated culture medium contains various organic reactive species. When Ringer's lactated solutions, containing sodium lactate ($\text{Na-C}_3\text{H}_5\text{O}_3$), sodium chloride (NaCl), potassium chloride (KCl), and calcium chloride (CaCl_2) are used, other organic substances that can kill cancer cells without killing normal cells are generated in the plasma-treated lactated solutions, called plasma-activated solutions (PAL) [63]. During the plasma treatments of the lactated solutions, a hydroxyl radical ($\bullet\text{OH}$) is generated and reacted with the alcohol moiety of the lactate skeleton. The $\bullet\text{CH-}$ and $\bullet\text{CH}_2-$ type radicals on the lactate skeleton are formed by the hydrogen abstraction due to the $\bullet\text{OH}$ radical. In aqueous chemistry, organic acids such as acetate, pyruvate, and glyoxylate are derived from decomposition and oxidation [64,65]. Moreover, dimerization occurs to form substances, such as 2,3-dimethyltratarate [66], and additive reactions create products containing methyl amine groups [67]. These examples exhibit rich chemistry in plasma-induced aqueous reactions, including the dehydration, esterification, hydrolysis, and dimerization of the original organic molecules.

In simplification, oxygen radicals are separated from the plasma source, without electrons, ions, and photons, and when oxygen radicals are irradiated into the solutions, bactericidal effects of the oxygen radical-treated solutions have been reported [68,69]. Recently, the bactericidal effects of L-Tryptophan (Trp)-containing solutions were reported, and the bactericidal effect was found [70]. After the oxygen radical irradiation, products, such as kynurenine and *N'*-formyl kynurenine, were observed to be stable in the solution. However, the bactericidal effect was obtained only by in situ irradiation with oxygen radicals. The in situ reactions form the short-lived tryptophan radical ($\text{Trp}\bullet$) that is an intermediate precursor for transformation from Trp to kynurenine reaction scheme [70]. The authors indicated that oxygen radical irradiation transformed organic fertilizer into a bactericide. Until now, short-lived species have not been a concern; however, controlled plasma-driven phenomena can be used as pharmaceutical drugs. There are no clear advantages and disadvantages of plasma-generated products, together with oxidative or reductive stimuli toward living organisms; the plasma pharmacy is irreplaceable and its low invasiveness precludes no alternative method.

4.3. Plasma Seed Science: Enhancement of Germination and Growth of Plant Seeds

Regarding the interactions between plasma and living organisms, the inactivation of pathogenic microorganisms, bacteria, and viruses has been observed after plasma treatment without damaging agricultural products [71]. Several studies have reported that direct plasma irradiation of plant seeds promotes germination and growth [72–74]. In the physiological process of seed germination [75], regulation of the balance of phytohormones, such as abscisic acid (ABA) and gibberellin (GA), stops dormancy, seed metabolism synthesizes enzymes, and seed germination occurs during seedling processes with regard to the softening of the cell wall and expansion of the shoot and root [76–79]. The mechanical properties of seeds change during physiological germination. Atmospheric pressure air plasma releases dormancy in *Arabidopsis thaliana* seeds and modifies the glass-to-rubber transition temperatures of seed coats [80]. Protein delay of germination 1 (DOG1) is the master regulator of seed dormancy, enhancing ABA signaling and interactions with phosphatases [81,82]. Seed dormancy 4 like 1 (SFL1) positively regulates the termination of the seed dormancy program [83].

In the other case, when the *A. thaliana* seeds are treated by low-pressure oxygen plasma, the expression of epigenetic-related genes of DME regulates DNA methylation and RNA-directed DNA methylation (RDM4). Epigenetic changes determine the production of enzymes that catalyze reactions regulating DNA demethylation and histones associated with the chromosomal region of the gene [84]. More recently, epigenetic regulation of methylation and acetylation of the DNA-promotor regions of ABA metabolism and α -amylase was altered by the plasma irradiation of rice seeds, and germination of heat-stressed seeds was restored [85] (Figure 6).

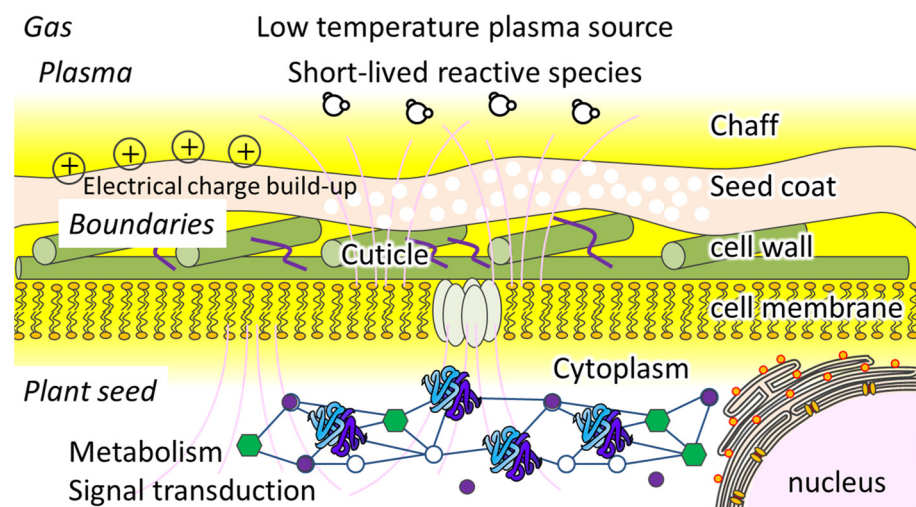


Figure 6. Plasma seed science. Elucidation of mechanisms of the epigenetic alternation of phenotypes of seeds due to a short-time plasma irradiation. Reactive species transport inside porous chaff and coats of seeds, and biochemical reactions may alter the methylation or acetylation of the cytosine base of DNA or the lysine residue of histones of nucleosomes.

Because seeds have a storage lifetime, their senescence leads to a decrease in germination rates. Seed color and radical concentrations measured by electron spin resonance (ESR) affect both the germination rate and plant growth [86]. High nitrate concentrations have been reported in plasma-treated seeds with no significant risks [87,88]. When plasma treatments were performed during the cultivation of rice plants in paddy fields, the quality of the rice seeds improved [89,90].

Plasma treatment plays an important role in biological stimulation. Stimuli above the normal level of organization are provided for short periods, leading to the chemical, biochemical, and biological responses observed in the relaxation process. Plasma triggers irreversible changes in dynamics. This behavior occurs as a chemical change based on

physical action. This response is a characteristic function of the amount of trigger stimulation, which is a low-dose stimulus that is harmful at high doses. Intense and short-lived stimuli act as coherent processes, resulting in a synergistic effect even at low doses.

5. Emergence of the Plasma-Driven Science Concept

All plasma-driven phenomena are categorized as a chain of plasma generation, a chemical reaction network with radical formation, and reactions at the surface and through the boundaries of multiple phases. These hierarchical interactions in plasma processing can be revisited and adapted for the evolution of plasma-driven science.

Plasma complexity arises from the interactions between complex systems. Plasma plays a role in instantaneous stimulation exceeding normal levels. Once the system is stimulated, its excited energy begins to decay via chemical relaxation, followed by chemical reaction networks. First, relaxation processes demonstrate the emergence of essential functions in chemical, biochemical, and biological responses. This phenomenon is known as plasma physical action and chemical relaxation (PACR) [59,60]. At the spatial scale, self-organized structures are constructed. This has been argued in examples of self-organization phenomena [91].

Chemical reactions are complex chain networks that describe topologically structured relationships among the nodes of detectable species. Venturi et al. reported a directed weighted graph for plasma chemistry characterization of negatively charged hydrogen ion sources [92]. Sakai et al. reported a cause-effect network for the plasma chemistry of silicon film deposition in SiH_4 and H_2 mixture plasma based on the connections between chemical reactants and products. Moreover, a network for CH_4 plasma chemistry was reported. The scale-free nature of the obtained network can be rescaled by reducing the number of nodes by selecting primary components [93–96]. The BCl_3 and H_2 plasma chemistry were provided by Hancinac et al. [97]

The temporal evolution and dynamic processes of a system response are difficult to understand. Comprehensive measurements must be performed on multiple particles in real-time, and the resulting effects on the system must be analyzed and characterized from multiple perspectives. The complex system of plasma physics-to-chemistry networks and systems represents the functions of a living organism. This is considered the result of system-to-system interactions. The complex system response must be understood in advance.

Living conditions are subject to temporal changes. Biological lifetime is not invariant to time reversal. Multiplications of events are moving toward the future by the change in events moving toward the past. This represents irreversible event changes. When the PACR occurs, complex structures and various reaction pathways arise in space and time. At equilibrium, the system reached its most stable state in terms of energy. For non-equilibrium plasma-driven phenomena, the structure is metastable and depends on what happened in the past events. This implies that the metastable state was memorized. Such a hysteresis, or memory, is one way of achieving a metastable state. This was an energy-related phenomenon. Schrödinger indicated that as the number of molecules decreases, the effect of fluctuations in the chemical reaction network increases, and statistically rare phenomena are more likely to occur. Similar to thermal hysteresis, differences in the heating and cooling processes indicate that different chemical structures of materials pass through different material states. As previously mentioned, ferroelectric materials exhibit permanent electric polarization, which can be reversed by applying a sufficiently strong electric field [98,99]. Furthermore, according to the ergodic hypothesis, temporal and spatial fluctuations were considered equal. Autocatalysis provides positive feedback that promotes the formation of specific reaction products. In a reaction that initiates and yields a product, the rate is proportional to the concentration of the starting reaction feedstock. In catalytic reactions, a spatially heterogeneous increase in reaction products or a higher reaction rate occurs when the reactant concentration increases. This is a chemical reaction network with positive feedback and is considered a type of memory effect.

To solve this complexity, comprehensive measurements of dynamic changes in structural networks with regard to plasma-driven phenomena should be performed, approaching both physics and chemistry.

6. Evolution and the Future of Plasma-Driven Sciences

These plasma interactions have a tremendous positive impact on society. For example, film deposition and material-etching processes have been developed for the atomic-scale manufacturing of semiconductor devices based on LTP technology [100–104]. In addition, methods for converting and synthesizing materials using the carbon or nitrogen cycle in the global circulation of materials have been discussed using plasma catalysis [105–107]. Further developments in plasma generation at biologically optimal temperatures have led to the emergence of plasma bio-applications, such as plasma medicine and plasma agriculture. Plasma treatments are currently considered as a tool of multiple stress inducers. The directly plasma-irradiated fission yeast was inhibited to proper cell separation, which is regulated by transcriptional target genes of *ace2* and *sep1*, and the target of rapamycin kinase complex 1 (TORC1). Mitotic progression was downregulated by plasma irradiation. By prevention of mother–daughter cell separation, multi-cellular aggregates or multicellularity is a factor contributing to stress tolerance [108].

There must be (i) development of plasma instrumentation, (ii) comprehensive measurements, and (iii) multiple integrated analytical approaches utilizing informatics (Figure 7). Since there is a wide variety of plasma-driven phenomena, including the unknown areas to date, there is a need to develop instrumentation or devices to mimic and construct naturally or artificially generated phenomena.

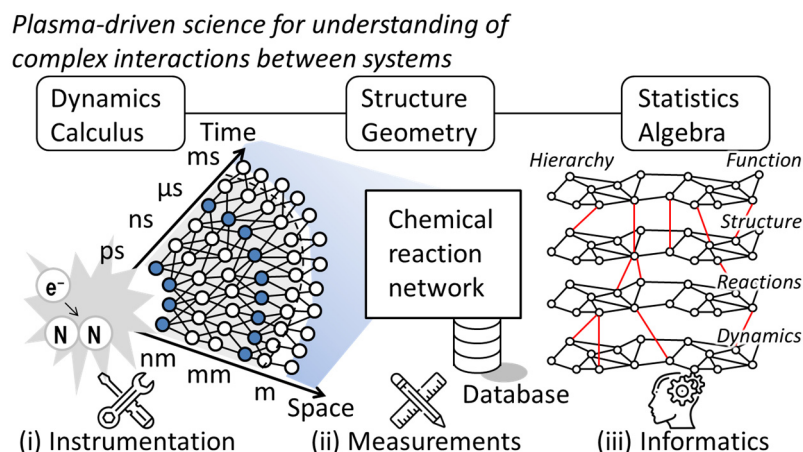


Figure 7. Perspectives on the plasma-driven science. Science-based, data-driven development of (i) instrumentation, (ii) measurement techniques, and (iii) informatics and data-driven analysis are required for understanding the complex interactions occurring in the plasma-driven phenomena. The mechanisms behind these phenomena will be elucidated and the interactions can be controlled for in situ functionalization of such plasma processes as plasma catalysis, plasma medicine, and plasma agriculture. The emergence and evolution of plasma-driven science and technology are newly addressed.

In detached recombining plasma, owing to unnatural situations occurring in the surrounding areas of the excited plasma region, abundant radical chemistry can occur, leading to tremendous effects on material synthesis. Therefore, the development of this area is critically important.

We must develop techniques to measure and monitor the non-equilibrium physical and chemical reaction fields generated by plasma, which are called plasma diagnostics [109]. Numerous experiments have been previously conducted. Although it is important to conduct trial-and-error experiments, accurate predictions may be possible if experimental

data based on reliable measurements in a well-defined experimental system are utilized in the future. Therefore, reliable measurement data in a well-defined experimental system enables the prediction of results using computational chemistry and theory building.

In recent years, rapid progress in computational environments, which have benefited from the development of LTP technology, has accelerated the demand for the accumulation of experimental and measurement data, and the construction of a virtual experimental environment is desired [110]. The systematic data harvesting and exploration to initiate a form of “plasma informatics” was identified in the low-temperature plasma science community with a comprehensive summary of science-based data-driven developments [110,111]. Data-driven plasma science was reviewed by Anirudh et al. [112]

The prediction of yields for the sputtering of single elements by monoenergetic monoatomic ion beams was performed by regression model analysis [113] of the experimental dataset provided by Yamamura et al. [114]. Kruger et al. reported that artificial neural networks (ANN) are trained based on machine learning of the sputter deposition of Ti–Al films [115]. They approached to solve this by dividing into multiple spatiotemporal scales for each interaction between the ion and solid-state surface (ps and nm), the formation of the electron (ns and microns), and its collision-induced formation of ions as heavy particles in bulk plasma ($> \mu\text{s}$ and $> \text{mm}$). Each physical process can be simulated using molecular dynamics code, an empirical kinetic Monte Carlo sputter model based on the impinging energy and incident angles, and particle-in-cell plasma codes. The training of the directed links of all the data from gas-phase to surface demonstrated the prediction of the complex sputtering process [115,116]. They also demonstrated ANN analysis for the sputtering of Al and AlN films [117,118].

Kamataki et al. reported a hybrid machine learning of classification and regression models for producing highly electrically conductive indium tin oxide (ITO) films. Plasma parameters can be optimized based on the search conditions for nitrogen-mediated amorphization using the incorporation of N atoms [119].

The ANN model was trained using a dataset measuring the optical emissions H (434.0, 486.1, and 656.3 nm) and O (777.4 and 844.6 nm) of the plasma generated on the liquid surface of the NaNO_3 solution [120]. The convolutional neural network was trained by classifying the volatile organics with their optical emission spectra involving lines for C_2 (468.0, 516.5, 668.5 nm), CH (431.4 nm), CN (388.3 nm), and OH (306.4 nm) in the range of 200–900 nm from the microplasma system [121,122]. The potential of machine learning with supervised or unsupervised training and testing for modeling, diagnostics, and control of plasma has also been discussed [123]. The machine-learning methods for the datasets of measurements, such as optical emission spectra, Fourier-transformed infrared spectra, current–voltage characteristics, and scanning electron microscope images, were reviewed by Bobzanini et al. [124]

Frankes et al. introduced the metadata scheme Plasma-MDS to facilitate published data by following the principles of findability, accessibility, interoperability, and reusability (FAIR). This scheme provides availability for entries of plasma sources, plasma media and targets, plasma diagnostics, and plasma dataset resources [125].

To understand the aforementioned plasma processes, the plasma parameters during these processes should be determined by in situ measurements and real-time monitoring. To unravel the complex system interactions, difficulty, and nonlinear behavior of a hierarchical complex system, informatics approaches to the huge amount of data known as big data, coupled with machine learning and neural networks, have recently become popular. The total set for the reaction system is governed by a non-Markov process and is non-deterministic. If the system variables can be divided into locally small systems, then the local system can be described by a Markov process and a deterministic, more predictable stochastic process. It is necessary to incorporate large elementary reactions and in situ data from multiple measurements and comprehensive analyses. Decisions regarding the time evolution of the systems may become possible within a short time and within a narrow space. Such complex phenomena need to be considered through informatics

approaches not only in terms of the electromagnetic interactions but also comprehensively with both natural and artificially generated phenomena.

7. Conclusions

In this review, we first explain the fundamentals of low-temperature plasma and focus on its non-linearity, hysteresis, and non-equilibrium nature. Various interactions exist between plasma and its targets. Interestingly, as plasma particles, such as electrons, ions, radicals, and photons, are generated, the excited plasma field changes into a chemistry-rich physicochemical reaction field. Detached plasma processes are irreversible and create various plasma-driven phenomena. Studies on plasma–liquid interactions have evolved beyond the functionalization of pharmaceutical effects and are called plasma pharmacies. The effect of plasma treatment on seed germination and plant growth opens up an emerging interdisciplinary field of plasma seed science. We emphasize the emergence and evolution of the research fields. Plasma-driven science should be promoted, which leads to the discovery of previously unseen phenomena, new laws triggered by plasma, and the creation of new plasma processes. The research goal should be the systematization of plasma processes and electronics in materials, environment, and life.

Author Contributions: Writing—original draft preparation, K.I.; writing—review and editing, K.K. and N.O. All authors have read and agreed to the published version of the manuscript.

Funding: This study was partially supported by JSPS-KAKENHI, grant numbers 21H04451, 20H00142, and 21H01073. The authors would like to thank the Center for low-temperature plasma science of Nagoya University for the joint usage/research program.

Data Availability Statement: Data is contained within the article.

Acknowledgments: The authors would like to thank Masaru Hori, Makoto Sekine, Masaharu Shiratani, Hiromasa Tanaka, and the Ishikawa-Tanaka laboratory members for fruitful discussions.

Conflicts of Interest: The authors declare no conflict of interest.

References

1. Alfvén, H.; Boley, F.I. Worlds-Antiworlds, Antimatter in Cosmology. *Am. J. Phys.* **1967**, *35*, 453–454. [[CrossRef](#)]
2. Alfvén, H. *Cosmology in the Plasma Universe, Lecture at the Institute of Space Research Academy of Sciences on Moscow*; TRITA-EPP-87-07: Trita, Peru, 1987; ISSN 0348-7539.
3. Langmuir, I. Oscillations in Ionized Gases. *Proc. Natl. Acad. Sci. USA* **1928**, *14*, 627–637. [[CrossRef](#)]
4. Tonks, L.; Langmuir, I. Oscillations in ionized gases. *Phys. Rev.* **1929**, *33*, 195. [[CrossRef](#)]
5. Hori, M. Radical controlled processes. *Rev Mod Plasma Phys.* **2022**, *6*, 36. [[CrossRef](#)]
6. Adamovich, I.; Agarwal, S.; Ahedo, E.; Alves, L.L.; Baalrud, S.; Babaeva, N.; Bogaerts, A.; Bourdon, A.; Bruggeman, P.J.; Canal, C.; et al. The 2022 Plasma roadmap: Low temperature plasma science and technology. *J. Phys. D* **2022**, *55*, 373001. [[CrossRef](#)]
7. Adamovich, I.; Baalrud, S.D.; Bogaerts, A.; Bruggeman, P.J.; Cappelli, M.; Colombo, V.; Czarnetzki, U.; Ebert, U.; Eden, J.G.; Favia, P.; et al. The 2017 Plasma Roadmap: Low temperature plasma science and technology. *J. Phys. D* **2017**, *50*, 323001. [[CrossRef](#)]
8. Samukawa, S.; Hori, M.; Rauf, S.; Tachibana, K.; Bruggeman, P.; Kroesen, G.; Whitehead, J.C.; Murphy, A.B.; Gutsol, A.F.; Starikovskaia, S.; et al. The 2012 Plasma Roadmap. *J. Phys. D* **2012**, *45*, 253001. [[CrossRef](#)]
9. Chen, F.F. *Introduction to Plasma Physics and Controlled Fusion*, 3rd ed.; Springer: Berlin/Heidelberg, Germany, 2015.
10. Lieberman, M.A.; Lichtenberg, A.J. *Principles of Plasma Discharges and Materials Processing*, 2nd ed.; Wiley Interscience: Hoboken, NJ, USA, 2005; p. 28.
11. Niemi, K.; Waskoenig, J.; Sadeghi, N.; Gans, T.; O’Connell, D. The role of helium metastable states in radio-frequency driven helium–oxygen atmospheric pressure plasma jets: Measurement and numerical simulation. *Plasma Sources Sci. Technol.* **2011**, *20*, 055005. [[CrossRef](#)]
12. Murakami, T.; Niemi, K.; Gans, T.; O’Connell, D.; Graham, W.G. Chemical kinetics and reactive species in atmospheric pressure helium–oxygen plasmas with humid-air impurities. *Plasma Sources Sci. Technol.* **2012**, *22*, 015003. [[CrossRef](#)]
13. Yoshimura, S.; Otsubo, Y.; Yamashita, A.; Ishikawa, K. Insights into normothermic treatment with direct irradiation of atmospheric pressure plasma for biological applications. *Jpn. J. Appl. Phys.* **2021**, *60*, 010502. [[CrossRef](#)]
14. Takamura, S. *Kyokai Ryoiki Plasma Riko Gaku No Kiso (in Japanese)*; Morikita Publishing Co., Ltd.: Tokyo, Japan, 2010; ISBN 10.4627784619.
15. Ohno, N. Plasma detachment in linear devices. *Plasma Phys. Control. Fusion* **2017**, *59*, 034007. [[CrossRef](#)]

16. Kallenbach, A.; Bernert, M.; Dux, R.; Reimold, F.; Wischmeier, M.; Team, A.U. Analytical calculations for impurity seeded partially detached divertor conditions. *Plasma Phys. Control. Fusion* **2016**, *58*, 045013. [[CrossRef](#)]
17. Perillo, R.; Chandra, R.A.; Akkermans, G.R.; Vijvers, W.A.J.; Graef, W.A.A.D.; Classen, I.G.J.; van Dijk, J.; de Baar, M.R. Studying the influence of nitrogen seeding in a detached-like hydrogen plasma by means of numerical simulations. *Plasma Phys. Control. Fusion* **2018**, *60*, 105004. [[CrossRef](#)]
18. Perillo, R.; Akkermans, G.; Classen, I.; Vijvers, W.; Chandra, R.; Jesko, K.; Korving, S.; Vernimmen, J.; de Baar, M. Experimental evidence of enhanced recombination of a hydrogen plasma induced by nitrogen seeding in linear device Magnum-PSI. *Nucl. Mater. Energy* **2019**, *19*, 87–93. [[CrossRef](#)]
19. Perillo, R. Plasma chemistry in divertor relevant plasmas. Ph.D. Thesis, Eindhoven University of Technology, Eindhoven, The Netherlands, 2017.
20. Ohno, N.; Ezumi, N.; Takamura, S.; Krasheninnikov, S.I.; Pigarov, A.Y. Experimental evidence of molecular activated recombination in detached recombining plasmas. *Phys. Rev. Lett.* **1998**, *81*, 818. [[CrossRef](#)]
21. Ohno, N.; Seki, M.; Ohshima, H.; Tanaka, H.; Kajita, S.; Hayashi, Y.; Natsume, H.; Takano, H.; Saeki, I.; Yoshikawa, M.; et al. Investigation of recombination front region in detached plasmas in a linear divertor plasma simulator. *Nucl. Mater. Energy* **2019**, *19*, 458–462. [[CrossRef](#)]
22. Ohshima, H.; Kajita, S.; Tanaka, H.; Ohno, N.; van der Meiden, H.J. Thomson scattering measurement of two electron temperature components in transition to detached plasmas. *Plasma Fusion Res.* **2018**, *13*, 1201099. [[CrossRef](#)]
23. Kajita, S.; Ohshima, H.; Tanaka, H.; Seki, M.; Takano, H.; Ohno, N. Spatial and temporal measurement of recombining detached plasmas by laser Thomson scattering. *Plasma Sources Sci. Technol.* **2019**, *28*, 105015. [[CrossRef](#)]
24. Kajita, S.; Suzuki, K.; Tanaka, H.; Ohno, N. Helium line emission spectroscopy in recombining detached plasmas. *Phys. Plasmas* **2018**, *25*, 063303. [[CrossRef](#)]
25. Kajita, S.; Akkermans, G.; Fujii, K.; van der Meiden, H.; van de Sanden, M.C.M. Emission spectroscopy of He lines in high-density plasmas in Magnum-PSI. *AIP Adv.* **2020**, *10*, 025225. [[CrossRef](#)]
26. Kajita, S.; Nishijima, D.; Fujii, K.; Akkermans, G.; van der Meiden, H.J. Application of multiple regression for sensitivity analysis of helium line emissions to the electron density and temperature in Magnum-PSI. *Plasma Phys. Control. Fusion* **2021**, *63*, 055018. [[CrossRef](#)]
27. Kajita, S.; Iwai, S.; Tanaka, H.; Nishijima, D.; Fujii, K.; van der Meiden, H.; Ohno, N. Use of machine learning for a helium line intensity ratio method in Magnum-PSI. *Nucl. Mater. Energy* **2022**, *33*, 101281. [[CrossRef](#)]
28. Nishijima, D.; Baldwin, M.J.; Chang, F.; Tynan, G.R. Machine learning-aided line intensity ratio technique applied to deuterium plasmas. *AIP Adv.* **2023**, *13*, 055202. [[CrossRef](#)]
29. Lin, K.; Goto, M.; Akatsuka, H. Improved line intensity analysis of neutral helium by incorporating the reabsorption processes in a helium collisional-radiative model. *Atoms* **2023**, *11*, 94. [[CrossRef](#)]
30. Onda, T.; Kajita, S.; Iijima, T.; Tonegawa, A.; Ohno, N.; Tanaka, H. Transverse motion of a plasma column in a sheet plasma. *Contrib. Plasma Phys.* **2017**, *57*, 87–93. [[CrossRef](#)]
31. Tanaka, H.; Kajita, S.; Natsume, H.; Saeki, I.; Ohno, N. Spatiotemporal dynamics of cross-field ejection events in recombining detached plasma. *Plasma Phys. Control. Fusion* **2020**, *62*, 075011. [[CrossRef](#)]
32. Thakur, S.C.; Simmonds, M.J.; Caneses, J.F.; Chang, F.-J.; Hollmann, E.M.; Doerner, R.P.; Goulding, R.H.; Lumsdaine, A.; Rapp, J.; Tynan, G.R. PISCES-RF: A liquid-cooled high-power steady-state helicon plasma device. *Plasma Sources Sci. Technol.* **2021**, *30*, 055014. [[CrossRef](#)]
33. Tanaka, H.; Hayashi, Y.; Kajita, S.; van der Meiden, H.J.; Yoshikawa, M.; Vernimmen, J.W.M.; Scholten, J.; Classen, I.; Morgan, T.W.; Ohno, N. Cross-field transport in detached helium plasmas in Magnum-PSI. *Plasma Phys. Control. Fusion* **2020**, *62*, 115021. [[CrossRef](#)]
34. Costin, C.; Mihaila, I.; van der Meiden, H.J.; Tanaka, H.; Scholten, J.; van Eck, H.J.N. Plasma rotation and axial flow velocities in Magnum-PSI from cross-correlation measurements. *Plasma Sources Sci. Technol.* **2023**, *32*, 075010. [[CrossRef](#)]
35. Ezumi, N.; Iijima, T.; Sakamoto, M.; Nakashima, Y.; Hirata, M.; Ichimura, M.; Perillo, R. Synergistic effect of nitrogen and hydrogen seeding gases on plasma detachment in the GAMMA 10/PDX tandem mirror. *Nucl. Fusion* **2019**, *59*, 066030. [[CrossRef](#)]
36. Hasegawa, H.; Tanaka, H.; Ishiguro, S. Linear analysis of cross-field dynamics with feedback instability on detached divertor plasmas. *Nucl. Fusion* **2021**, *61*, 126055. [[CrossRef](#)]
37. Okamoto, T.; Ezumi, N.; Togo, S.; Perillo, R.; Shigematsu, N.; Seto, T.; Takanashi, K.; Takahashi, S.; Miyauchi, R.; Sakamoto, M. Effect of impurity ions on ion current flowing into an ion sensitive probe during N₂ and H₂ seeding in hydrogen plasma. *Plasma Fusion Res.* **2023**, *18*, 1402047. [[CrossRef](#)]
38. Tanaka, H.; Saeki, I.; Ohno, N.; Kajita, S.; Ido, T.; Natsume, H.; Hatayama, A.; Hoshino, K.; Sawada, K.; Goto, M. Detached helium plasma simulation by a one-dimensional fluid code with detailed collisional-radiative model. *Phys. Plasmas* **2020**, *27*, 102505. [[CrossRef](#)]
39. Tanaka, H.; Ezumi, N.; Sugiyama, T.; Gamo, H.; Shigematsu, N.; Yoshikawa, M.; Sakamoto, M. Study of the intermittent plasma structure around the divertor simulation experimental module in GAMMA 10/PDX. *Phys. Plasma* **2023**, *30*, 032501. [[CrossRef](#)]
40. Nagase, M.; Masuda, H.; Ohno, N.; Takamura, S.; Takagi, M. High density plasma generation by RF ohmic discharge in toroidal divertor simulator NAGDIS-T. *J. Nucl. Mater.* **2007**, *363–365*, 611–615. [[CrossRef](#)]

41. Yada, K.; Matsui, N.; Ohno, N.; Kajita, S.; Takamura, S.; Takagi, M. Investigation of detached recombining deuterium plasma and carbon chemical erosion in the toroidal divertor simulator NAGDIS-T. *J. Nucl. Mater.* **2009**, *390-391*, 290–294. [[CrossRef](#)]
42. Ohno, N.; Takamura, S. Bridge between Fusion Plasma and Plasma Processing. *J. Plasma Fusion Res.* **2008**, *84*, 740. (In Japanese)
43. Asaoka, K.; Ohno, N.; Hayashi, Y.; Kajita, S.; Tanaka, H. Generation of spiral shape nitrogen recombining plasma for atomic nitrogen source. *Plasma Fusion Res.* **2019**, *14*, 3401069. [[CrossRef](#)]
44. Kumar, A.; Caneses-Marin, J.; Lau, C.; Goulding, R. Parallel transport modeling of linear divertor simulators with fundamental ion cyclotron heating. *Nucl. Fusion* **2023**, *63*, 036004. [[CrossRef](#)]
45. Islam, M.S.; Nakashima, Y.; Hatayama, A.; Ishiguro, S.; Hoshino, K.; Ezumi, N.; Sakamoto, M. Study of end-cell plasma parameters of GAMMA 10/PDX by the LINDA code. *Plasma Phys. Contrib. Fusion* **2019**, *61*, 125005. [[CrossRef](#)]
46. Takizuka, T. Kinetic effects in edge plasma: Kinetic modeling for edge plasma and detached divertor. *Plasma Phys. Control. Fusion* **2017**, *59*, 34008. [[CrossRef](#)]
47. Stangeby, P.C. Basic physical processes and reduced models for plasma detachment. *Plasma Phys. Control. Fusion* **2018**, *60*, 044022. [[CrossRef](#)]
48. Kanazawa, S.; Kogoma, M.; Moriwaki, T.; Okazaki, S. Stable glow plasma at atmospheric pressure. *J. Phys. D* **1988**, *21*, 838–840. [[CrossRef](#)]
49. Yokoyama, T.; Kogoma, M.; Kanazawa, S.; Moriwaki, T.; Okazaki, S. The improvement of the atmospheric-pressure glow plasma method and the deposition of organic films. *J. Phys. D* **1990**, *23*, 374–377. [[CrossRef](#)]
50. Yokoyama, T.; Kogoma, M.; Moriwaki, T.; Okazaki, S. The mechanism of the stabilisation of glow plasma at atmospheric pressure. *J. Phys. D* **1990**, *23*, 1125. [[CrossRef](#)]
51. Okazaki, S.; Kogoma, M.; Uehara, M.; Kimura, Y. Appearance of stable glow discharge in air, argon, oxygen and nitrogen at atmospheric pressure using a 50 Hz source. *J. Phys. D* **1993**, *26*, 889–892. [[CrossRef](#)]
52. Okazaki, S.; Kogoma, M. Development of atmospheric pressure glow discharge plasma and its application on a surface with curvature. *J. Photopolym Sci. Technol.* **1993**, *6*, 339. [[CrossRef](#)]
53. Ishikawa, K.; Takeda, K.; Yoshimura, S.; Kondo, T.; Tanaka, H.; Toyokuni, S.; Nakamura, K.; Kajiyama, H.; Mizuno, M.; Hori, M. Generation and measurement of low-temperature plasma for cancer therapy: A historical review. *Free. Radic. Res.* **2023**, *57*, 239–270. [[CrossRef](#)]
54. Pigarov, A.; Krashennnikov, S. Application of the collisional-radiative, atomic-molecular model to the recombining divertor plasma. *Phys. Lett. A* **1996**, *222*, 251–257. [[CrossRef](#)]
55. Kim, H.-H.; Teramoto, Y.; Ogata, A.; Takagi, H.; Nanba, T. Plasma catalysis for environmental treatment and energy applications. *Plasma Chem. Plasma Process.* **2016**, *36*, 45–72. [[CrossRef](#)]
56. Kim, H.; Teramoto, Y.; Ogata, A.; Takagi, H.; Nanba, T. Atmospheric-pressure nonthermal plasma synthesis of ammonia over ruthenium catalysts. *Plasma Process. Polym.* **2016**, *14*, 1600157. [[CrossRef](#)]
57. Rouwenhorst, K.H.R.; Kim, H.-H.; Lefferts, L. Vibrationally excited activation of N₂ in plasma-enhanced catalytic ammonia synthesis: A kinetic analysis. *ACS Sustain. Chem. Eng.* **2019**, *7*, 17515–17522. [[CrossRef](#)]
58. Teramoto, Y.; Kim, H.-H. Effect of vibrationally excited N₂(ν) on atomic nitrogen generation using two consecutive pulse corona discharges under atmospheric pressure N₂. *J. Phys. D* **2019**, *52*, 494003. [[CrossRef](#)]
59. Kaneko, T.; Kato, H.; Yamada, H.; Yamamoto, M.; Yoshida, T.; Attri, P.; Koga, K.; Murakami, T.; Kuchitsu, K.; Ando, S.; et al. Functional nitrogen science based on plasma processing: Quantum devices, photocatalysts and activation of plant defense and immune systems. *Jpn. J. Appl. Phys.* **2022**, *61*, SA0805. [[CrossRef](#)]
60. Ishikawa, K. Perspectives on functional nitrogen science and plasma-based in situ functionalization. *Jpn. J. Appl. Phys.* **2022**, *61*, SA0802. [[CrossRef](#)]
61. Tanaka, H.; Ishikawa, K.; Mizuno, M.; Toyokuni, S.; Kajiyama, H.; Kikkawa, F.; Metelmann, H.-R.; Hori, M. State of the art in medical applications using non-thermal atmospheric pressure plasma. *Rev. Mod. Plasma Phys.* **2017**, *1*, 1–89. [[CrossRef](#)]
62. Ishikawa, K.; Reuter, S. Physical and chemical basis of nonthermal plasma. In *Plasma Medical Science*; Academic Press: Cambridge, MA, USA, 2019.
63. Tanaka, H.; Nakamura, K.; Mizuno, M.; Ishikawa, K.; Takeda, K.; Kajiyama, H.; Utsumi, F.; Kikkawa, F.; Hori, M. Non-thermal atmospheric pressure plasma activates lactate in Ringer's solution for anti-tumor effects. *Sci. Rep.* **2016**, *6*, 36282. [[CrossRef](#)]
64. Liu, Y.; Ishikawa, K.; Tanaka, H.; Miron, C.; Kondo, T.; Nakamura, K.; Hori, M. Organic decomposition and synthesis reactions in lactated solution exposed to non-equilibrium atmospheric pressure plasma. *Plasma Process Polym.* **2023**, *20*, 2200193. [[CrossRef](#)]
65. Miron, C.; Ishikawa, K.; Kashiwagura, S.; Suda, Y.; Tanaka, H.; Nakamura, K.; Kajiyama, H.; Toyokuni, S.; Mizuno, M.; Hori, M. Cancer-specific cytotoxicity of Ringer's acetate solution irradiated by cold atmospheric pressure plasma. *Free. Radic. Res.* **2023**, *57*, 91–104. [[CrossRef](#)]
66. Tanaka, H.; Hosoi, Y.; Ishikawa, K.; Yoshitake, J.; Shibata, T.; Uchida, K.; Hashizume, H.; Mizuno, M.; Okazaki, Y.; Toyokuni, S.; et al. Low temperature plasma irradiation products of sodium lactate solution that induce cell death on U251SP glioblastoma cells were identified. *Sci. Rep.* **2021**, *11*, 18488. [[CrossRef](#)]
67. Ito, D.; Iwata, N.; Ishikawa, K.; Nakamura, K.; Hashizume, H.; Miron, C.; Tanaka, H.; Kajiyama, H.; Toyokuni, S.; Mizuno, M.; et al. Cytotoxicity of plasma-irradiated lactate solution produced under atmospheric airtight conditions and generation of the methyl amino group. *Appl. Phys. Express* **2022**, *15*, 056001. [[CrossRef](#)]

68. Kobayashi, T.; Iwata, N.; Oh, J.S.; Hahizume, H.; Ohta, T.; Takeda, K.; Ito, M. Bactericidal pathway of Escherichia coli in buffered saline treated with oxygen radicals. *J. Phys. D* **2017**, *50*, 155208. [[CrossRef](#)]
69. Iwata, N.; Gamaleev, V.; Hashizume, H.; Oh, J.; Ohta, T.; Ishikawa, K.; Hori, M.; Ito, M. Simultaneous achievement of antimicrobial property and plant growth promotion using plasma-activated benzoic compound solution. *Plasma Process. Polym.* **2019**, *16*, 1900023. [[CrossRef](#)]
70. Iwata, N.; Ishikawa, K.; Nishikawa, Y.; Kato, H.; Shimizu, M.; Kato, M.; Hori, M. Oxygen radical irradiation transforms an organic fertilizer L-tryptophan into an environment and human-friendly bactericide. *Environ. Technol. Innovation* **2024**, *33*, 103496. [[CrossRef](#)]
71. Ito, M.; Ohta, T.; Hori, M. Plasma agriculture. *J. Korean Phys. Soc.* **2012**, *60*, 937. [[CrossRef](#)]
72. Koga, K.; Thapanut, S.; Amano, T.; Seo, H.; Itagaki, N.; Hayashi, N.; Shiratani, M. Simple method of improving harvest by nonthermal air plasma irradiation of seeds of *Arabidopsis thaliana* L. *Appl. Phys. Express* **2016**, *9*, 016201. [[CrossRef](#)]
73. Attri, P.; Ishikawa, K.; Okumura, T.; Koga, K.; Shiratani, M. Plasma agriculture from laboratory to farm: A review. *Processes* **2020**, *8*, 1002. [[CrossRef](#)]
74. Xi, D.-K.; Yap, S.L.; Kumar, N.N.; Toh, C.C.; Ishikawa, K.; Hori, M. Plasma-assisted priming: Improved germination and seedling performance of papaya. *Sains Malays.* **2023**, *52*, 599–611. [[CrossRef](#)]
75. Bewley, J.D.; Bradford, K.; Hilhorst, H. *Seeds: Physiology of Development, Germination and Dormancy*, 3rd ed.; Springer: Berlin/Heidelberg, Germany, 2013.
76. Grainge, G.; Nakabayashi, K.; Iza, F.; Leubner-Metzger, G.; Steinbrecher, T. Gas-plasma-activated water impact on photo-dependent dormancy mechanisms in nicotiana tabacum seeds. *Int. J. Mol. Sci.* **2022**, *23*, 6709. [[CrossRef](#)]
77. Grainge, G.; Nakabayashi, K.; Steinbrecher, T.; Kennedy, S.; Ren, J.; Iza, F.; Leubner-Metzger, G. Molecular mechanisms of seed dormancy release by gas plasma-activated water technology. *J. Exp. Bot.* **2022**, *73*, 4065–4078. [[CrossRef](#)]
78. Steinbrecher, T.; Leubner-Metzger, G. The biomechanics of seed germination. *J. Exp. Bot.* **2016**, *68*, 765–783. [[CrossRef](#)]
79. Nakabayashi, K.; Walker, M.; Irwin, D.; Cohn, J.; Guida-English, S.M.; Garcia, L.; Pavlović, I.; Novák, O.; Tarkowská, D.; Strnad, M.; et al. The phytotoxin myrigalone a triggers a phased detoxification programme and inhibits lepidium sativum seed germination via multiple mechanisms including interference with auxin homeostasis. *Int. J. Mol. Sci.* **2022**, *23*, 4618. [[CrossRef](#)] [[PubMed](#)]
80. August, J.; Dufour, T.; Bailly, C. Release of Arabidopsis seed dormancy by cold atmospheric plasma relies on cytoplasmic glass transition. *J. Phys. D* **2023**, *56*, 415202. [[CrossRef](#)]
81. Née, G.; Kramer, K.; Nakabayashi, K.; Yuan, B.; Xiang, Y.; Miatton, E.; Finkemeier, I.; Soppe, W.J.J. Delay of germination1 requires PP2C phosphatases of the ABA signalling pathway to control seed dormancy. *Nat. Commun.* **2017**, *8*, 72. [[CrossRef](#)] [[PubMed](#)]
82. Nishimura, N.; Tsuchiya, W.; Moresco, J.J.; Hayashi, Y.; Satoh, K.; Kaiwa, N.; Irisa, T.; Kinoshita, T.; Schroeder, J.I.; Yates, J.R., III; et al. Control of seed dormancy and germination by DOG1-AHG1 PP2C phosphatase complex via binding to heme. *Nat. Commun.* **2018**, *9*, 2132. [[CrossRef](#)] [[PubMed](#)]
83. Zheng, L.; Otani, M.; Kanno, Y.; Seo, M.; Yoshitake, Y.; Yoshimoto, K.; Kawakami, N. Seed dormancy 4 like1 of Arabidopsis is a key regulator of phase transition from embryo to vegetative development. *Plant J.* **2022**, *112*, 460. [[CrossRef](#)]
84. Ahmed, S.; Khanom, S.; Hayashi, N. Persistence of growth enhancement induced by oxygen plasma irradiation seed and leaf. *Agronomy* **2023**, *13*, 1579. [[CrossRef](#)]
85. Suriyasak, C.; Hatanaka, K.; Tanaka, H.; Okumura, T.; Yamashita, D.; Attri, P.; Koga, K.; Shiratani, M.; Hamaoka, N.; Ishibashi, Y. Alterations of DNA methylation caused by cold plasma treatment restore delayed germination of heat-stressed rice (*Oryza sativa* L.) seeds. *ACS Agric. Sci. Technol.* **2021**, *1*, 5–10. [[CrossRef](#)]
86. Attri, P.; Ishikawa, K.; Okumura, T.; Koga, K.; Shiratani, M.; Mildaziene, V. Impact of seed color and storage time on the radish seed germination and sprout growth in plasma agriculture. *Sci. Rep.* **2021**, *11*, 2539. [[CrossRef](#)]
87. Okumura, T.; Attri, P.; Kamataki, K.; Yamashita, N.; Tsukada, Y.; Itagaki, N.; Koga, K. Detection of NO₃⁻ introduced in plasma-irradiated dry lettuce seeds using liquid chromatography-electrospray ionization quantum mass spectrometry (LC-ESI QMS). *Sci. Rep.* **2022**, *12*, 12525. [[CrossRef](#)]
88. Okumura, T.; Tanaka, H.; Nakao, T.; Anan, T.; Arita, R.; Shiraki, M.; Shiraki, K.; Miyabe, T.; Yamashita, D.; Matsuo, K.; et al. Health assessment of rice cultivated and harvested from plasma-irradiated seeds. *Sci. Rep.* **2023**, *13*, 17450. [[CrossRef](#)]
89. Hashizume, H.; Kitano, H.; Mizuno, H.; Abe, A.; Yuasa, G.; Tohno, S.; Tanaka, H.; Ishikawa, K.; Matsumoto, S.; Sakakibara, H.; et al. Improvement of yield and grain quality by periodic cold plasma treatment with rice plants in a paddy field. *Plasma Process. Polym.* **2020**, *18*, 2000181. [[CrossRef](#)]
90. Hashizume, H.; Kitano, H.; Mizuno, H.; Abe, A.; Yuasa, G.; Tohno, S.; Tanaka, H.; Ishikawa, K.; Matsumoto, S.; Sakakibara, H.; et al. Efficacy of periodic cold plasma treatment in a paddy to produce white-core grains in brewer's rice cultivar Yamadanishiki. *Free. Radic. Res.* **2023**, *57*, 161–173. [[CrossRef](#)]
91. Nicolis, G.; Prigogine, I. *Self-Organization in Nonequilibrium Systems: From Dissipative Structures to Order Through Fluctuations*; Wiley: Hoboken, NJ, USA, 1977.
92. Venturi, S.; Yang, W.; Kaganovich, I.; Casey, T. An uncertainty-aware strategy for plasma mechanism reduction with directed weighted graphs. *Phys. Plasmas* **2023**, *30*, 043904. [[CrossRef](#)]
93. Murakami, T.; Sakai, O. Rescaling the complex network of low-temperature plasma chemistry through graph-theoretical analysis. *Plasma Sources Sci. Technol.* **2020**, *29*, 115018. [[CrossRef](#)]

94. Sakai, O.; Nobuto, K.; Miyagi, S.; Tachibana, K. Analysis of weblike network structures of directed graphs for chemical reactions in methane plasmas. *AIP Adv.* **2015**, *5*, 107140. [CrossRef]
95. Mizui, Y.; Kojima, T.; Miyagi, S.; Sakai, O. Graphical classification in multi-centrality-index diagrams for complex chemical networks. *Symmetry* **2017**, *9*, 309. [CrossRef]
96. Sakai, O.; Kawaguchi, S.; Murakami, T. Complexity visualization, dataset acquisition, and machine-learning perspectives for low-temperature plasma: A review. *Jpn. J. Appl. Phys.* **2022**, *61*, 070101. [CrossRef]
97. Hanicinec, M.; Mohr, S.; Tennyson, J. A regression model for plasma reaction kinetics. *J. Phys. D* **2023**, *56*, 374001. [CrossRef]
98. Yamaguchi, M.; Arisawa, M.; Shigeno, M.; Saito, N. Equilibrium and nonequilibrium chemical reactions of helicene oligomers in the noncovalent bond formation. *Bull. Chem. Soc. Jpn.* **2016**, *89*, 1145–1169. [CrossRef]
99. Yamaguchi, M. Thermal hysteresis involving reversible self-catalytic reactions. *Accounts Chem. Res.* **2021**, *54*, 2603–2613. [CrossRef] [PubMed]
100. Sekine, M. Dielectric film etching in semiconductor device manufacturing—Development of SiO₂ etching and the next generation plasma reactor. *Appl. Surf. Sci.* **2022**, *192*, 270. [CrossRef]
101. Ishikawa, K.; Karahashi, K.; Ichiki, T.; Chang, J.P.; George, S.M.; Kessels, W.M.M.; Kinoshita, K. Progress and prospects in nanoscale dry processes: How can we control atomic layer reactions? *Jpn. J. Appl. Phys.* **2017**, *56*, 06HA02. [CrossRef]
102. Ishikawa, K.; Karahashi, K.; Ishijima, T.; Cho, S.I.; Elliott, S.; Hausmann, D.; Kinoshita, K. Progress in nanoscale dry processes for fabrication of high-aspect-ratio features: How can we control critical dimension uniformity at the bottom? *Jpn. J. Appl. Phys.* **2018**, *57*, 06JA01. [CrossRef]
103. Iwase, T.; Kamaji, Y.; Kang, S.Y.; Koga, K.; Kuboi, N.; Nakamura, M.; Negishi, N.; Nozaki, T.; Nunomura, S.; Ogawa, D.; et al. Progress and perspectives in dry processes for nanoscale feature fabrication: Fine pattern transfer and high-aspect-ratio feature formation. *Jpn. J. Appl. Phys.* **2019**, *58*, SE0802. [CrossRef]
104. Ishikawa, K.; Ishijima, T.; Shirafuji, T.; Armini, S.; Despiau-Pujo, E.; Gottscho, R.A.; Kanarik, K.J.; Leusink, G.J.; Marchack, N.; Murayama, T.; et al. Rethinking surface reactions in nanoscale dry processes toward atomic precision and beyond: A physics and chemistry perspective. *Jpn. J. Appl. Phys.* **2019**, *58*, SE0801. [CrossRef]
105. Nozaki, T.; Okazaki, K. Non-thermal plasma catalysis of methane: Principles, energy efficiency, and applications. *Catal. Today* **2013**, *211*, 29–38. [CrossRef]
106. Sheng, Z.; Kim, H.-H.; Yao, S.; Nozaki, T. Plasma-chemical promotion of catalysis for CH₄ dry reforming: Unveiling plasma-enabled reaction mechanisms. *Phys. Chem. Chem. Phys.* **2020**, *22*, 19349–19358. [CrossRef]
107. Kim, D.-Y.; Ham, H.; Chen, X.; Liu, S.; Xu, H.; Lu, B.; Furukawa, S.; Kim, H.-H.; Takakusagi, S.; Sasaki, K.; et al. Cooperative catalysis of vibrationally excited CO₂ and alloy catalyst breaks the thermodynamic equilibrium limitation. *J. Am. Chem. Soc.* **2022**, *144*, 14140–14149. [CrossRef]
108. Otsubo, Y.; Yamashita, A.; Goto, Y.; Sakai, K.; Iida, T.; Yoshimura, S.; Johzuka, K. Cellular responses to compound stress induced by atmospheric-pressure plasma in fission yeast. *J. Cell. Sci.* **2023**, *136*, jcs261292. [CrossRef]
109. Ishikawa, K. *Plasma diagnostics, In Cold Plasma in Food and Agriculture, Fundamentals and Applications*; Academic Press: Cambridge, MA, USA, 2016.
110. Kambara, M.; Kawaguchi, S.; Lee, H.J.; Ikuse, K.; Hamaguchi, S.; Ohmori, T.; Ishikawa, K. Science-based, data-driven developments in plasma processing for material synthesis and device-integration technologies. *Jpn. J. Appl. Phys.* **2023**, *62*, SA0803. [CrossRef]
111. Trieschmann, J.; Vialletto, L.; Gergs, T. Machine learning for advancing low-temperature plasma modeling and simulation. *J. Micro Nanopattern. Mater. Metrol.* **2023**, *22*, 041504.
112. Anirudh, R.; Archibald, R.; Asif, M.S.; Becker, M.M.; Benkadda, S.; Bremer, P.-T.; Budé, R.H.S.; Chang, C.S.; Chen, L.; Churchill, R.M.; et al. 2022 Review of Data-Driven Plasma Science. *IEEE Trans. Plasma Sci.* **2023**, *51*, 1750–1838. [CrossRef]
113. Kino, H.; Ikuse, K.; Dam, H.C.; Hamaguchi, S. Characterization of descriptors in machine learning for data-based sputtering yield prediction. *Phys. Plasma* **2021**, *28*, 013504. [CrossRef]
114. Yamamura, Y.; Itikawa, Y.; Itoh, N. Angular dependence of sputtering yields of monatomic solids. Report No IPPJ-AM-26. Available online: <http://dpc.nifs.ac.jp/IPPJ-AM/IPPJ-AM-32.pdf> (accessed on 28 December 2023).
115. Krüger, F.; Gergs, T.; Trieschmann, J. Machine learning plasma-surface interface for coupling sputtering and gas-phase transport simulations. *Plasma Sources Sci. Technol.* **2019**, *28*, 035002. [CrossRef]
116. Gergs, T.; Borislavov, B.; Trieschmann, J. Efficient plasma-surface interaction surrogate model for sputtering processes based on autoencoder neural networks. *J. Vac. Sci. Technol. B* **2021**, *40*, 012802. [CrossRef]
117. Gergs, T.; Mussenbrock, T.; Trieschmann, J. Physics-separating artificial neural networks for predicting initial stages of Al sputtering and thin film deposition in Ar plasma discharges. *J. Phys. D* **2023**, *56*, 084003. [CrossRef]
118. Gergs, T.; Mussenbrock, T.; Trieschmann, J. Physics-separating artificial neural networks for predicting sputtering and thin film deposition of AlN in Ar/N₂ discharges on experimental timescales. *J. Phys. D* **2023**, *56*, 194001. [CrossRef]
119. Kamataki, K.; Ohtomo, H.; Itagaki, N.; Lesly, C.F.; Yamashita, D.; Okumura, T.; Shiratani, M. Prediction by a hybrid machine learning model for high-mobility amorphous In₂O₃:Sn films fabricated by RF plasma sputtering deposition using a nitrogen-mediated amorphization method. *J. Appl. Phys.* **2023**, *134*, 163301. [CrossRef]

120. Wang, C.; Ko, T.; Hsu, C. Machine learning with explainable artificial intelligence vision for characterization of solution conductivity using optical emission spectroscopy of plasma in aqueous solution. *Plasma Process. Polym.* **2021**, *18*, e2100096. [[CrossRef](#)]
121. Wang, C.-Y.; Ko, T.-S.; Hsu, C.-C. Interpreting convolutional neural network for real-time volatile organic compounds detection and classification using optical emission spectroscopy of plasma. *Anal. Chim. Acta* **2021**, *1179*, 338822. [[CrossRef](#)] [[PubMed](#)]
122. Zhang, X.-L.; Hsu, C.-C. Using transfer-learning-based algorithms as data reduction strategies for volatile organic compounds classification using plasma spectroscopy. *J. Phys. D* **2023**, *56*, 324003. [[CrossRef](#)]
123. Mesbah, A.; Graves, D.B. Machine learning for modeling, diagnostics, and control of non-equilibrium plasmas. *J. Phys. D* **2019**, *52*, 30LT02. [[CrossRef](#)]
124. Bonzanini, A.D.; Shao, K.; Graves, D.B.; Hamaguchi, S.; Mesbah, A. Foundations of machine learning for low-temperature plasmas: Methods and case studies. *Plasma Sources Sci. Technol.* **2023**, *32*, 024003. [[CrossRef](#)]
125. Franke, S.; Paulet, L.; Schäfer, J.; O'connell, D.; Becker, M.M. Plasma-MDS, a metadata schema for plasma science with examples from plasma technology. *Sci. Data* **2020**, *7*, 439. [[CrossRef](#)]

Disclaimer/Publisher's Note: The statements, opinions and data contained in all publications are solely those of the individual author(s) and contributor(s) and not of MDPI and/or the editor(s). MDPI and/or the editor(s) disclaim responsibility for any injury to people or property resulting from any ideas, methods, instructions or products referred to in the content.